Magnetic and electronic properties of the $LaNi_{5-x}Al_x$ system

2002 J. Phys.: Condens. Matter 14 8057

(http://iopscience.iop.org/0953-8984/14/34/324)

INSTITUTE OF PHYSICS PUBLISHING JOURNAL OF PHYSICS: CONDENSED MATTER

J. Phys.: Condens. Matter **14** (2002) 8057–8065 PII: S0953-8984(02)33604-X

Magnetic and electronic properties of the $LaNi_{5-x}Al_x$ system

E Burzo[1,4], S G Chiuzbăian[2], M Neumann[2] and L Chioncel[3]

[1] Faculty of Physics, Babeş-Bolyai University, RO-3400 Cluj, Napoca, Romania
[2] Fachbereich Physik, Universität Osnabrück, D-49069 Osnabrück, Germany
[3] Department of Physics, University of Nijmegen, N-6500GL Nijmegen, The Netherlands

Received 8 February 2002, in final form 18 June 2002
Published 15 August 2002
Online at stacks.iop.org/JPhysCM/14/8057

Abstract

Magnetic measurements performed on the $LaNi_{5-x}Al_x$ system show that the magnetic susceptibilities increase up to a temperature T_{max}, characteristic for each composition. In the temperature range $T \leqslant 10$ K, a T^2-dependence of the magnetic susceptibilities was evidenced for compositions $x = 0$ and 1. In the high-temperature range the magnetic susceptibilities were analysed as a superposition of a Pauli-paramagnetic term on a Curie–Weiss-type contribution. The effective nickel moments decrease with increasing Al content. X-ray photoelectron spectroscopy measurements and band structure calculations show that the Fermi level is gradually shifted to a region with lower density of states when Al is substituted for Ni. The magnetic behaviour of nickel was analysed in correlation with the sample composition.

1. Introduction

The physical properties of RNi_5 compounds where R is a rare earth were studied in connection with their ability to absorb large quantities of hydrogen [1–3]. Many substitutions were made, particularly on Ni sites, in order to analyse the hydrogen storage capacity, the plateau pressure and the kinetics [4–6]. In this context, the crystal structures of $RNi_{5-x}Al_x$ with R = Nd, Gd [5], Er [6], Dy [7] were studied. It was shown that for $x < 2$ the pseudo-binary systems form solid solutions having hexagonal $CaCu_5$-type structure ($P6/mmm$ space group). For $2 < x \leqslant 3$ the structure changes to a $HoNi_{2.6}Ga_{2.4}$-type one. This structure is also hexagonal, with space group $P6/mmm$, having a larger unit cell than the $CaCu_5$ one. The unit-cell parameters of the two types of structure are related by $a_{HoNi_{2.6}Ga_{2.4}} = \sqrt{3}a_{CaCu_5}$ and $c_{HoNi_{2.6}Ga_{2.4}} = c_{CaCu_5}$ [5]. In $CaCu_5$-type structure, the Al substitution takes place at the 3g sites situated in the $z = 1/2$ plane which does not contain R atoms [5]. This site allows greater d_{Ni-Al} distances. Total filling of the 3g sites by Al is not possible since the distances between Ni and Al or Al and Al are smaller than the sum of metallic radii $r_{Ni} + r_{Al}$ or $r_{Al} + r_{Al}$ and thus a structure change

[4] Author to whom any correspondence should be addressed.

0953-8984/02/348057+09$30.00

appears. The occurrence of $HoNi_{2.6}Ga_{2.4}$ superstructure induces an increase of the Al 3f–Ni 6k and Al 3f–Al 6k distances, making the possibility to locate aluminium in the 3f and 6k sites. In this structure, Ni occupies completely 6l sites and Al 3f sites. The 6k sites are statistically occupied by Ni and Al.

There are only few data concerning the magnetic and electronic properties of $LaNi_5$-based pseudo-binary systems [3]. In a previous paper [8] we reported the magnetic and electronic properties of the $LaNi_{5-x}Cu_x$ system. It was shown that there is a weak hybridization between Ni and Cu d states. The magnetic behaviour of nickel in the above system was analysed in the spin fluctuation model.

As part of an on-going work on the $LaNi_5$-based system we studied the $LaNi_{5-x}Al_x$ pseudo-binary compounds. In addition to crystal structure analysis and magnetic studies, x-ray photoelectron spectroscopy (XPS) measurements were performed. The experimental data were compared with those obtained from band structure calculations.

2. Experimental and computing methods

$LaNi_{5-x}Al_x$ samples with $x \leqslant 3$ were prepared in an induction furnace in a purified argon atmosphere. These were re-melted several times to ensure a good homogeneity. A small excess of La (<1%) was added to compensate for weight loss during melting. The samples were thermally treated under vacuum, at 1000 °C, for one week. The x-ray analysis showed the presence of only one phase having $CaCu_5$-type structure in the composition range $x \leqslant 2$. For sample with $x = 3$, a $HoNi_{2.6}Ga_{2.4}$-type structure was shown.

The magnetic measurements were performed in the temperature range 1.7–300 K and fields up to 9 T. For each temperature the magnetic susceptibility has been determined from magnetization isotherms, according to a Honda–Arrott plot [10]: $\chi = \chi_p + cM_sH^{-1}$ by extrapolating the measured values to $H^{-1} \to 0$. Here c denotes a presumed magnetic ordered impurity content and M_s is their saturation magnetization. By this method, any possible alteration of susceptibilities as a result of the presence of small quantities of magnetic ordered phase is avoided. The samples were generally shown to be free from magnetic impurities. A very small content of magnetic ordered phase (<0.1%) was evidenced, in some cases, only at very low temperatures. These can increase the magnetic susceptibilities by up to 20% if the above corrections are not considered.

The XPS measurements were performed using a PHI 5600ci Multitechnique system. The spectra were recorded at room temperature using monochromatized Al Kα radiation (1486.6 eV). The total energy resolution, as determined at the Fermi level of a gold foil, was about 0.3–0.4 eV. Binding energies are given with reference to the Fermi level. The $4f_{7/2}$ level of gold was found at 84.0 eV binding energy. The samples were fractured in the preparation chamber. All spectra were recorded in a vacuum below 5×10^{-10} mbar. The fractured samples contained only tiny amounts of oxygen and carbon.

Band structure calculations were carried out by using the *ab initio* tight-binding linear muffin-tin orbitals method in the atomic sphere approximation (TB-LMTO-ASA). The detailed procedure of calculations was described elsewhere [11–13]. In the framework of the local density approximation (LDA), the total electronic potential is the sum of external, Coulomb and exchange–correlation potentials [14]. The functional form of the exchange–correlation energy used in the present work was the free-electron gas parametrization of von Barth and Hedin [15]. Relativistic corrections are included without the spin–orbit coupling. For band structure calculations, the Al in the $CaCu_5$-type structure ($x \leqslant 2$) was located in 3g sites and in the $HoNi_{2.6}Ga_{2.4}$-type structure the Al was considered to occupy 3f and 6k sites as determined from crystal structure refinement [5]. Ni is located in 6l positions.

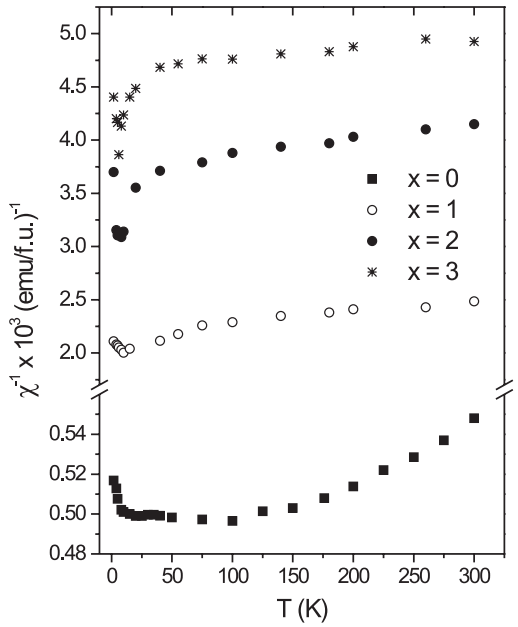

Figure 1. Thermal variations of reciprocal susceptibilities.

3. Experimental data

3.1. Magnetic measurements

The temperature dependences of the magnetic susceptibilities are plotted in figure 1. The data previously reported for $LaNi_5$ were also included [8]. The magnetic susceptibilities increase up to a characteristic temperature T_{max}. The T_{max}-values are shifted to lower temperatures with increasing aluminium content. Thus, for $x = 0$, $T_{max} \simeq 90$ K and then decreases to 12 K ($x = 1$), 8 K ($x = 2$) and 6 K ($x = 3$). Above $T^* = 150$ K, the reciprocal susceptibilities for $LaNi_5$ follow a Curie–Weiss-type behaviour. For aluminium-doped samples, above a characteristic temperature T^*, which decreases from $T^* = 20$ K ($x = 1$) to 10 K ($x = 3$), the magnetic susceptibilities can be described as a superposition of a Pauli-paramagnetic term, χ_0, on a Curie–Weiss-type contribution:

$$\chi = \chi_0 + C(T - \theta)^{-1}. \tag{1}$$

We denoted by C the Curie constant and θ is the paramagnetic Curie temperature. The values of C, χ_0 and θ obtained by fitting the experimental data are listed in table 1. The Pauli-type contributions increase with increasing aluminium content. The paramagnetic Curie temperatures are negative and decrease in absolute magnitude with increasing x. The effective nickel moments determined from Curie constants are very sensitive to aluminium content, decreasing from 2.15 μ_B/atom ($x = 0$) to 0.72 μ_B/atom ($x = 1$), 0.27 μ_B/atom for $x = 2$ and 0.18 μ_B/atom for $x = 3$.

In the low-temperature range ($T \leqslant 10$ K) the magnetic susceptibilities, for compounds with $x = 0$ and 1, follow a T^2-dependence—figure 2:

$$\chi = \chi_0(1 + aT^2) \tag{2}$$

with $a = 1.3 \times 10^{-3}$ K^{-2} for the sample having $x = 0$ and 0.23×10^{-3} K^{-2} for the $LaNi_4Al$ compound.

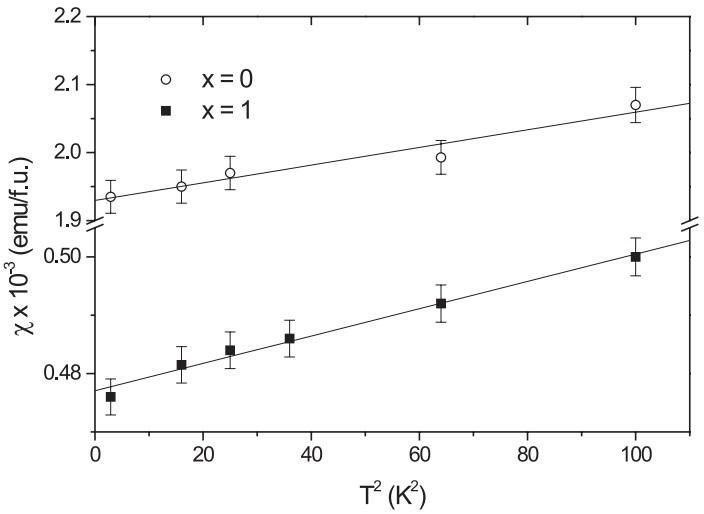

Figure 2. Temperature dependences of the magnetic susceptibilities for $LaNi_{5-x}Al_x$ with $x = 0$ and 1 at $T \leqslant 10$ K.

Table 1. Data obtained from magnetic measurements on the $LaNi_{5-x}Al_x$ system.

x	M_{eff}(Ni) (μ_B/atom)	$\chi_0 \times 10^4$ (emu/fu)	C (emu K/fu)	$-\theta$ (K)	T_{max} (K)	$a \times 10^3$ (K^{-2}) Experiment	Calculation
0	2.15	—	2.850	1104	90	1.30	1.22
1	0.72	1.00	0.260	650	12	0.23	0.17
2	0.27	1.80	0.028	240	8	—	—
3	0.18	1.85	0.008	220	6	—	—

Since the temperatures T_{max} are very low for compounds with aluminium content higher than $x \geqslant 2$, it was not possible to analyse the temperature dependence of their magnetic susceptibilities in the low-temperature region.

3.2. XPS measurements

The Ni $2p_{3/2}$, $2p_{1/2}$ and La $3d_{3/2}$ core-level lines are presented in figure 3. Due to the overlapping of the Ni $2p_{3/2}$ line with the La $3d_{3/2}$ one, no accurate determination of the Ni positions can be made. A fit was performed by taking it into account that the sharp peak must correspond to the Ni $2p_{3/2}$ line. The binding energies determined, in the limit of experimental errors, seem to be not dependent on aluminium content. A characteristic feature of the spectra is the gradual vanishing of the Ni 6 eV satellite when alloying with Al; for samples with $x > 1$ it cannot be observed. The small peak at about 855 eV was attributed to the presence of a small quantity of lanthanum oxide. It results from oxygen adsorption on the surface after cleaving the samples in the preparation chamber.

The XPS valence bands recorded for the $LaNi_{5-x}Al_x$ samples and pure Ni are presented in figure 4. The computed densities of states, plotted also in the above figures, describe rather well the general features of experimental spectra. The orbital-projected partial densities of states were multiplied with the appropriate cross-sections for 1486.6 eV incident radiation

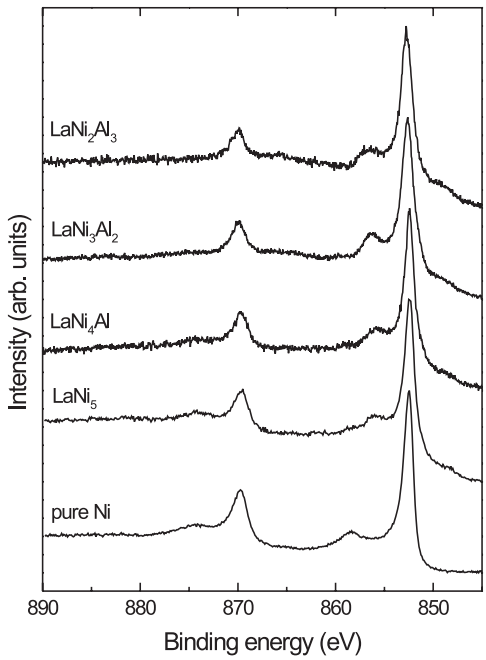

Figure 3. The Ni $2p_{3/2}$, $2p_{1/2}$ and La $3d_{3/2}$ core lines for the $LaNi_{5-x}Al_x$ system.

(Ni 3d: 0.59×10^{-2} Mb, Ni 4s: 0.83×10^{-3} Mb, La 5d: 0.76×10^{-3} Mb, La 6s: 0.29×10^{-3} Mb, Al 3p: 0.59×10^{-4} Mb from [9]) and their sum was then convoluted with Lorentzians of half-width 0.4 eV. There are also some differences. These can be attributed to the fact that band structures were calculated at 0 K and those obtained by XPS were recorded at room temperature. In addition, d–d correlation effects were not considered in computing the density of states. Also, the inelastic scattering background present in the XPS spectra was not subtracted.

Analysing the XPS spectra, a similarity of the Ni 3d band for pure Ni and that of $LaNi_5$ can be seen. This fact evidences that the valence band of $LaNi_5$ is mainly derived from Ni 3d. The structure at about 6.0 eV binding energy is the well known Ni satellite. The intensity of satellites decreases and cannot be observed for compositions $x \geqslant 2$. The contribution of the La states to the valence band of $LaNi_5$ is not visible in the spectra. The reasons are the small contribution to the DOS, as observed from computed partial densities of states, and the low cross-section of lanthanum.

Alloying with Al induced changes in the Ni 3d band. The density of states at the Fermi level is diminished as compared with pure nickel and the maxima of the valence bands are shifted to higher binding energy. These shifts increase from 0.59 eV in pure Ni to $\simeq$0.67 eV in $LaNi_5$ and 0.80 eV in $LaNi_4Al$. In $LaNi_3Al_2$ the shift is by 1.60 eV and in $LaNi_2Al_3$ by 1.74 eV. The states at the Fermi level have mainly d character in $LaNi_5$. On alloying with aluminium, the s–p contribution to the DOS at the Fermi level increases. There is a diminution of d-electron correlations and the exchange enhancement factors decrease.

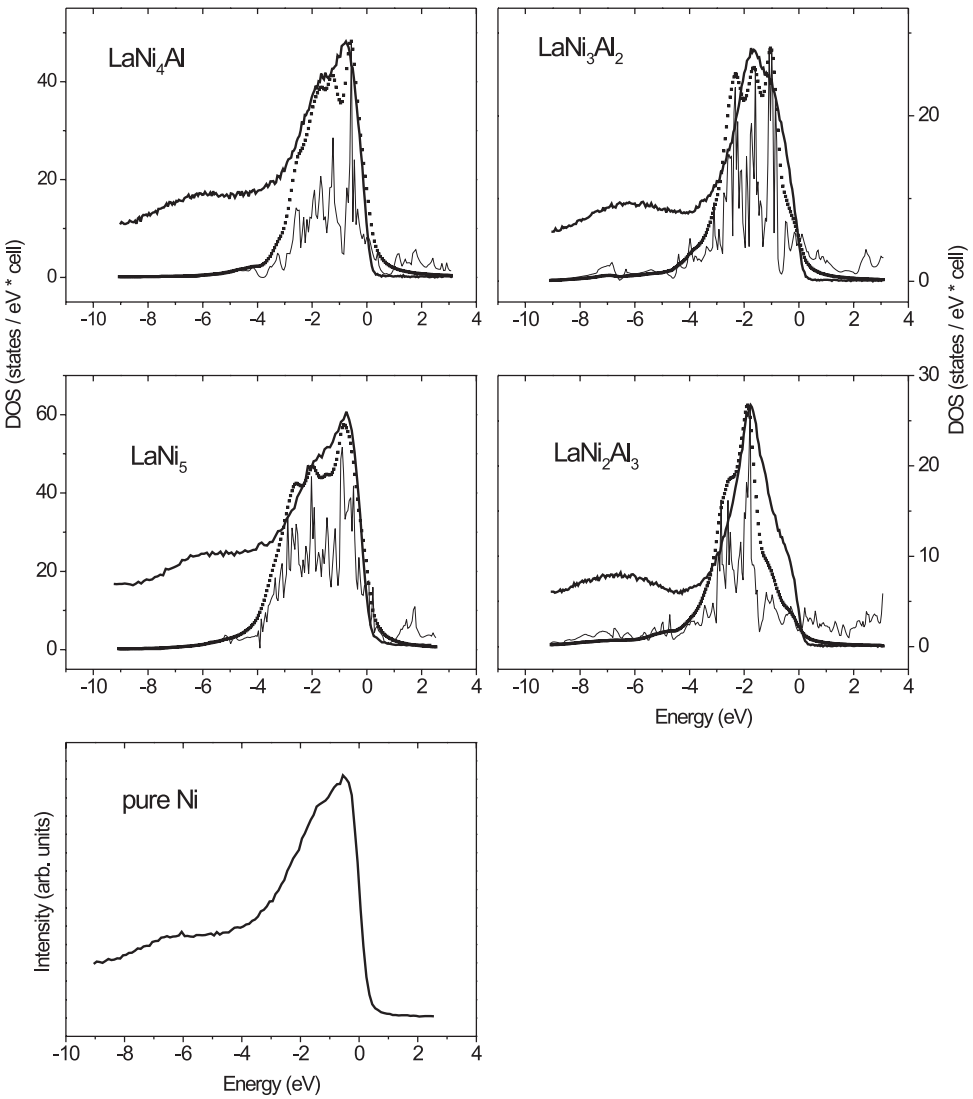

Figure 4. Comparison of the measured XPS valence bands (thick solid curve), the calculated total DOS (solid curve) and the convoluted DOS (with Lorentzians of half-width 0.4 eV and taking into account appropriate cross-sections for partial bands with different l-symmetry; dotted curve) for $LaNi_{5-x}Al_x$.

4. Discussion

The magnetic susceptibilities, in the low-temperature range, for $LaNi_5$ and $LaNi_4Al$, show T^2-dependence. For all samples studied the susceptibilities increase as a function of temperature up to a value located at T_{max} and then decrease. Above a characteristic temperature T^*, the presence of Curie–Weiss contributions which decrease on increasing aluminium content and are very weak for compositions $x \geqslant 2$ may be observed.

The above features may be analysed in framework of models which take into account the electron correlation effects in d bands such as the spin fluctuation model [16] or

dynamical mean-field theory (DMFT) [17]. These models reconcile the dual character of the electron, which as a particle requires a real-space description and as a wave requires a momentum-space description. Moriya [16] developed the concept of temperature-induced moments by considering the balance between the frequencies of longitudinal and transverse spin fluctuations. For an exchange-enhanced paramagnet, such as $LaNi_5$, the wavenumber-dependent susceptibility, χ_q, shows a relatively large enhancement due to electron–electron interactions, for small q-values. The temperature dependence of χ_q is significant only for these q-values. The average amplitude of local spin fluctuations $\langle S_{loc}^2 \rangle = 3k_B T \sum_q \chi_q$ is a temperature-dependent quantity, increasing until it reaches an upper limit, at a temperature T^*. At $T > T^*$ the system behaves as if it has local moments. The moments are localized in q-space. If the spin fluctuations are saturated, as in systems having very high exchange enhancement factors, s, the effective moments reflect the electron configuration of a 3d ion. As an example, for RCo_2 (R = Lu, Y) compounds, values of 3.87 μ_B/Co atom were determined, corresponding to the Co^{2+} electron configuration [18, 19]. In $LaNi_5$, since there are smaller exchange enhancement factors, $\langle S_{loc}^2 \rangle$ is not saturated, as shown by the effective Ni moment (2.15 μ_B) which is smaller as compared to that of the Ni^{2+} ion, considering only spin contributions (2.82 μ_B).

The experimental data for $LaNi_5$ maybe also analysed in the DMFT combined with standard LDA band calculations [20]. In a weakly correlated system, the local spin susceptibility is expected to be nearly temperature independent, while in a strongly correlated system, dominant Curie–Weiss behaviour at high temperatures is expected. For an itinerant electron system, the τ-dependence of the correlation function results in temperature dependence of $\langle S_{loc}^2 \rangle$. Fluctuating moments and atomic-like configuration are large at short times. The moment is reduced at longer timescales, corresponding to a more band-like and less correlated electronic structure near the Fermi level.

As for Ni, the presence of a 6 eV satellite was evidenced in the Ni 2p core lines for $LaNi_5$. The origin of this satellite is a matter of debate. Non-zero values of the Ni moment or inter-band d-electron hopping mechanism were previously considered. Recently, by using a numerically exact quantum scheme in the LDA + DMFT was possible to reproduce the 6 eV satellite in the DOS spectrum of Ni at $T = 0.9\ T_c$ [20]. This satellite was shown to have substantially more spin-up contributions.

When replacing Ni gradually by Al, there is a gradual hybridization of the Ni 3d band with Al s–p states and a diminution of the electron correlations. As result there is a decrease of the exchange enhancement factors. The Ni contributions to the Curie constants are smaller and, in addition, there is an increase of the Pauli-paramagnetic terms. These changes are very important for compositions with $x > 1$. In the case of $LaNi_3Al_2$ the effective nickel moment is only 0.27 μ_B and it nearly vanishes for $LaNi_2Al_3$. The gradual changes of the Ni 3d band configurations are also evidenced by the XPS spectra and band structure calculations. The intensity of the 6 eV satellite in the Ni 2p core line for $LaNi_5$ is smaller than that for pure nickel and vanishes for $LaNi_{5-x}Al_x$ for compositions $x \geqslant 2$. The maxima in the XPS valence band spectra shift to higher binding energy. We note that in the case of the non-magnetic $CeNi_2Al_3$ compound, the maximum of the valence band was shifted to 1.92 eV [21], a value somewhat greater than that evidenced for $LaNi_2Al_3$. The nickel is nearly non-magnetic or even actually non-magnetic in $LaNi_2Al_3$ and $LaNi_3Al_2$ as evidenced by magnetic measurements. The small temperature-dependent contributions to the susceptibilities, in the above samples, may be also considered as the result of the presence of small clusters of nickel atoms. If this mechanism is operative, quantities smaller than 1% of Ni atoms are situated in clusters as a result of non-random Al substitutions on 6k sites. The Al substitution is probably—but not in all cases—random, although the samples were careful prepared.

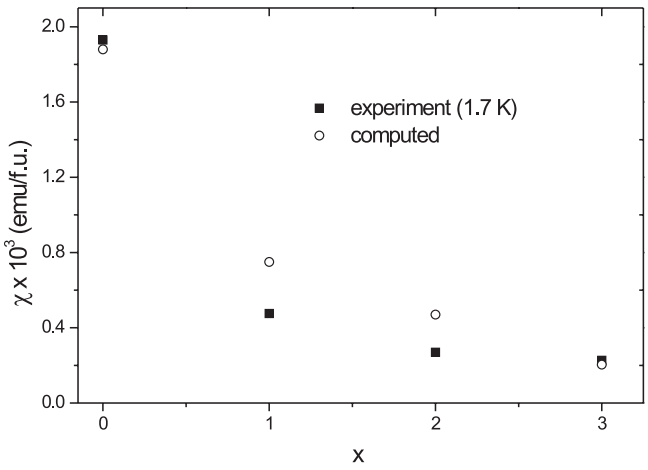

Figure 5. Composition dependences of the susceptibilities, at 1.7 K, and those obtained from band structure calculations.

By using the computed density of states we evaluated the magnetic susceptibilities at 0 K. These are in rather good agreement with the experimentally determined values at 1.7 K—figure 5. From the band structures we also determined the temperature factor, a, of the magnetic susceptibilities (equation (2)) in the low-temperature range, according to the relation [22]

$$a = \frac{\pi^2}{6}\left[\left(2\frac{N''(E_F)}{N(E_F)} - 1.2\frac{N'(E_F)^2}{N(E_F)^2}\right)\right]s^2 \tag{3}$$

where $N(E_F)$, $N'(E_F)$, $N''(E_F)$ are the density of states at the Fermi level and their first and second derivatives, respectively. We selected a symmetric energy interval around the self-consistent value of the Fermi level, and we used a mean square interpolation scheme in order to analytically evaluate the energy dependence of the density of states. This approach allowed us to evaluate the first and the second derivative of the DOS at the Fermi level. The values determined agree reasonable with those determined experimentally—table 1.

We conclude that in the $LaNi_{5-x}Al_x$ system there is a transition from a magnetic behaviour characterized by temperature-induced moments to a Pauli-type paramagnetism on increasing the aluminium content. This behaviour was correlated with the gradual hybridization of Ni 3d bands and diminution of d-electron correlations.

References

[1] Buschow K H J and van Mal H H 1972 *J. Less-Common Met.* **29** 203
[2] Diaz H, Percheron-Guegan A, Achard J C, Cattilon C and Mathieu J C *Proc. 2nd World Hydrogen Energy Conf.* p 111
[3] Burzo E, Chelkovski A and Kirchmayr H R 1990 *Landolt–Börnstein Handbook* vol 19f2 (Berlin: Springer)
[4] Takeshita T, Malik S K and Wallace W E 1978 *J. Solid State Chem.* **23** 271
[5] Bobet J L, Pechev S, Chevalier B and Darriet B 1998 *J. Alloys Compounds* **267** 136
[6] Sorgic B, Drasner A and Blazina Z 1996 *J. Alloys Compounds* **232** 79
[7] Sorgic B, Drasner A and Blazina Z 1995 *J. Phys.: Condens. Matter* **7** 7209
[8] Burzo E, Chiuzbăian S G, Chioncel L and Neumann M 2000 *J. Phys.: Condens. Matter* **12** 5897
[9] Yeh J J and Lindau I 1985 *At. Data Nucl. Data Tables* **32** 1
[10] Bates L 1951 *Modern Magnetism* (Cambridge: Cambridge University Press) p 133
[11] Andersen O K 1975 *Phys. Rev.* B **12** 3060
[12] Andersen O K and Jepsen O 1984 *Phys. Rev.* **53** 2571

[13] Andersen O K, Jepsen O and Glötzel D 1985 *Highlights of Condensed-Matter Theory* ed F Bassani, F Fumi and M P Tosi (New York: North-Holland)
[14] Jones R O and Gunnarson O 1989 *Rev. Mod. Phys.* **61** 689
[15] Von Barth U and Hedin L 1972 *J. Phys. C: Solid State Phys.* **5** 1629
[16] Moriya T 1991 *J. Magn. Magn. Mater.* **100** 201
[17] Georges A, Kotliar G, Krauth W and Rozenberg M J 1996 *Rev. Mod. Phys.* **68** 13
[18] Burzo E, Gratz E and Pop V 1993 *J. Magn. Magn. Mater.* **123** 159
[19] Burzo E, Givord D and Chioncel L 1998 *J. Appl. Phys.* **83** 1779
[20] Lichtenstein A I, Katsnelson M I and Kotliar G 2001 *Phys. Rev. Lett.* **87** 067205
[21] Coldea M, Neumann M, Pop V and Demeter M 2001 *J. Alloys Compounds* **323–324** 431
[22] Béal Monod M T 1982 *Physica* B **109–110** 1837